Journal of Materials Chemistry B

Rapid and direct MALDI-MS identification of pathogenic bacteria from blood via ionic liquid-modified magnetic nanoparticles (Fe3O4@SiO2)

Journal:	*Journal of Materials Chemistry B*
Manuscript ID:	TB-ART-04-2014-000528.R1
Article Type:	Paper
Date Submitted by the Author:	20-Apr-2014
Complete List of Authors:	Mukesh, Bhaisare; National Sun Yat-Sen University, Chemistry Abdelhamid, Hani; NSYSU, chemistry department Wu, Bosumg; NSYSU, Wu, Hui Fen; National Sun Yat-Sen University,

Rapid and direct MALDI-MS identification of pathogenic bacteria from blood via ionic liquid-modified magnetic nanoparticles (Fe_3O_4@SiO_2)

Mukesh L. Bhaisare[1§], Hani Nasser Abdelhamid[1, 2§], Bo-Sgum Wu[1], and Hui-Fen Wu[1, 3, 4, 5,6*]

[1]Department of Chemistry, National Sun Yat-Sen University, Kaohsiung, 70, Lien-Hai Road, Kaohsiung, 80424, Taiwan
[2]Department of Chemistry, Assuit University, Assuit, 71515, Egypt
[3]School of Pharmacy, College of Pharmacy, Kaohsiung Medical University, Kaohsiung, 806, Taiwan
[4]Institute of Medical Science and Technology, National Sun Yat-Sen University, 80424, Taiwan
[5]Doctoral Degree Program in Marine Biotechnology, National Sun Yat-Sen University, Kaohsiung, 80424, Taiwan
[6]Center for Nanoscience and Nanotechnology, National Sun Yat-Sen University, 70, Lien-Hai Road, Kaohsiung, 80424, Taiwan
*Corresponding author, Phone: +886-7-5252000-3955; Fax: +886-7-5253908
E-mail: hwu@faculty.nsysu.edu.tw (Prof. H.F.Wu)
[§]The authors (co-first authors) contributed equally to this work

Abstract

A novel method for pathogenic bacteria identification directly from blood samples by cationic ionic liquid-modified magnetic nanoparticle (CILMS) was reported. The magnetic nanoparticles were prepared by co-precipitation and the core-shell Fe_3O_4@SiO_2 nanoparticles were prepared by the sol-gel process, followed by the grafting of 3-chloropropyltrimethoxysilane that was reacted further with N-methylimidazole to form cationic ionic liquid-modified Fe_3O_4@SiO_2 magnetic nanoparticles (CILMS). The pathogenic bacteria were separated based on the electrostatic interactions among the negative charges of the cell membranes and the positive charges of the CILMS particles. CILMS is used directly without the need for any further apparatus and auxiliary chemicals. The separated cells were detected using matrix assisted laser desorption/ionization mass spectrometry (MALDI-MS). The lowest detectable number of bacteria was 3.4×10^3, 3.2×10^3, and 4.2×10^3 cfu mL^{-1} for *Escherichia coli*, *Pseudomonas aeruginosa*, and *Staphylococcus aureus*, respectively. The bacteria affinities toward CILMS were investigated using transmission electron microscopy that revealed immobilization of the CILMS on the outer of cell membranes. The present approach offers a high sensitivity, fast, and simple method for the cell capture of the pathogenic bacteria. The current

approach could be adapted to separate and identify the pathogenic bacteria from septicemic patients or contaminated blood before blood transfusions.

Keywords Magnetic nanoparticles; matrix assisted laser desorption/ionization mass spectrometry; pathogenic bacteria; separation; ionic liquid

1. Introduction

Pathogenic bacteria, among many others pathogens, account for many illnesses and epidemic diseases worldwide and are considered as high serious health threats. Bacteremia, the presence of bacteria in the bloodstream, has a high mortality rate (2850%). For instance, *Staphylococcus aureus (S. aureus*) is one of the top five pathogens that contribute to the most foodborne illnesses in America (www.cdc.gov, 2012). Thus, a rapid and accurate detection of pathogens in the bloodstream is vital for an effective prevention of severe health problems and can cause a great significance in diagnostics, and proteomics. [1-5] Nanoparticles, with large contact surface area and fast response, exhibit excellent capture efficiency due to the advantages of high surface/volume ratios and kinetics in reactivity, receiving much attention among the potential materials.[6] For the specificity and sensitivity of target bacteria, some affinity ligands were tailored on the surface of nanoparticle to generate affinity probes for the isolation of bacteria. Among the existing protocols, magnetic nanoparticles have received more attention because of their unique characteristics, such as facile preparation, good dispersion, facile post-modifications, good biocompatibility, and effective binding of biomacromolecules. As for the concerns of separation from reaction medium and the recyclability of materials, the separation and identification of pathogenic bacteria by magnetic nanoparticle (MNPs) has been achieved.[1-3, 7-25] Magnetic separation is a popular method which has many advantages such as simplicity, cheap, sensitive, and has the potential for further modification.

Ionic liquid-modified magnetic nanoparticles (IL-MNPs) have been received intensive attention recently for different applications such as catalysis,[26-29] dye removal,[30, 31] biomedical applications,[32]

biomolecular sensors,[33] and separation of biological materials.[34] It has been gained widespread popularity due to the advantages of thermal/chemical stability, ionic conductivity, highly responsiveness toward magnetic fields. Compared to the conventional magnetic nanoparticles, the aggregations almost were absent due to the repulsion of the same charges. Thus, it has high stability over than the modified magnetic nanoparticles. Several modifications have been made onto the surfaces of MNPs. However, non-specific bonding or decreasing trapping of pathogens have been encountered when these materials were used.[35-38]

Herein, we aim from this work to fabricate the ionic liquid-modified Fe_3O_4@SiO_2 magnetic nanoparticles for trapping the pathogenic bacteria and for rapid identification the pathogens using direct MALDI-MS analysis. On the surface of silica coated magnetite nanoparticles, 3-chloropropyltrimethoxysilane was anchored and N-methylimidazole to form cationic ionic liquid magnetic nanoparticles@silicate (CILMS) was grafted as the probe for pathogens. Since, silica possesses excellent physical properties such as large specific surface area and high stability; it was selected as ideally coating material. Compared to the magnetic beads, the application of IL-MNPs eradicates the pretreatment process of samples and mechanical mixing steps. Data revealed that pathogenic bacteria can be separated effectively from blood samples. The cell membrane affinities toward CILMS were further investigated using transmission electron microscopy (TEM) that indicate localization of the CILMS on the cell membrane

2. Experimental

2.1 Materials and instrumentation

Ferric chloride hexahydrate ($FeCl_3 \cdot 6H_2O$) was obtained from Showa Chemical Co. LTD (Japan), ammonium hydroxide (NH_4OH, 28%), tetraethylorthosilicate (TEOS) were purchased from Fluka (Steinheim Germany), triethylamine (TEA), choloropropyl (CP), sinapinic acid (SA), N-methylimidazole, 3-chloropropyltrimethoxysilane were purchased from Sigma-Aldrich (USA),

concentrated hydrochloric acid (HCl, 37.5%), toluene were obtained from Riedel-de Haën (Germany), ferrous chloride tetrahydrate ($FeCl_2 \cdot 4H_2O$) obtained from Alfa Aesar, Johnson Matthey Company (USA). All reagents used in the preparation process were of analytical reagent grade and without further purification.

The bacteria *Staphylococcus aureus* (BCRC 10451), *Escherichia coli* (BCRC 12570), and *Pseudomonas aeruginosa* (BCRC 10303) were cultivated at 37 °C and maintained on DifcoTM Nutrient Agar plates. The standard microdilution procedure was used for bacterial colony counting.

Matrix-assisted laser desorption/ionization mass spectrometry (MALDI-MS) analysis was performed by employing positive and linear mode on a time-of-flight mass spectrometer (Microflex, Daltonics Bruker, Bremen, Germany) with a 1.25 m flight tube. Desorption/ionization was obtained by using a nitrogen laser (337 nm) with a 3 ns pulse width. The accelerating potential in the source was maintained at +20 kV. All MALDI-MS spectra were obtained at the average of 200 laser shots. The laser power was adjusted to slightly above the ionization threshold of the cell lysate to obtain significant resolution signal-to-noise ratios and minimize the ionization suppression. The dried droplet method was used for all experiments using sinapinic acid as the matrix. To check the repeatability, all experimental results were repeated at least three times and reproducibility was confirmed using different cells and different fields. The Fourier transform infrared (FT-IR) spectra of magnetic nanoparticles were recorded on a FT-IR spectrometer (Spectrum 100, Perkin Elmer, USA). The morphology of the synthesized nanoparticles was determined by a transmission electron microscopy (TEM, Phillip CM200, Switzerland) at accelerating voltage 200 kV.

2.2 Preparation of magnetic nanoparticles

Magnetic nanoparticle (Fe_3O_4) was prepared using co-precipitation of ferrous and ferric salts. Typically,$FeCl_2 \cdot 4H_2O$ (0.63 g) and $FeCl_3 \cdot 6H_2O$ (1.73 g) were dissolved in 25 mL of double distilled water, then 40 mL of ammonia solution (28%) was added dropwisely prior to precipitation.[39] The

solution was purged with nitrogen and stirred in a water bath at 90 ºC for 3 h. The magnetic nanoparticles were separated using an external magnet and washed three times before use.

2.3 Synthesis of silica coated magnetic microspheres (Fe_3O_4@SiO_2)

The magnetic nanoparticle modified silica dioxide (SiO_2) was synthesized using the sol-gel approach. Initially, Fe_3O_4 nanoparticles (0.1 g) were treated with HCl (50 mL, 1 M) and were ultra-sonicated for 10 min. This treatment is important for better coating of Fe_3O_4 surface by silica layer. Then, the nanoparticles were separated and washed with deionized water. Magnetic nanoparticles were dispersed in the mixture of 160 mL ethanol and 40 mL deionized water, followed by the addition of concentrated ammonia aqueous solution (28 wt%, 6.0 mL). TEOS (300 mL) was diluted by 20 mL ethanol and then was added dropwisely into the reaction system and agitated for 5 h at room temperature. The solution of Fe_3O_4@SiO_2 was neutralized rapidly by adding HCl to avoid the formation of large clusters during separation by a magnet. The product was washed repeatedly with ethanol and water by the assistance of magnets, and then dried under vacuum at 70 ºC for 12 h.

2.4 Synthesis of the cationic ionic liquid-modified Fe_3O_4@SiO_2 magnetic nanoparticle (CILMS)

The amount of 0.4 g Fe_3O_4@SiO_2 was suspended in 150 mL of dry toluene and then an excess of 3-chloropropyltrimethoxysilane (4 mL) was added, followed by the addition of 1 mL triethylamine as catalyst. The suspension was stirred and reflux for 48 h under inert conditions using N_2 gas. After refluxing, the reaction was discontinued and the modified Fe_3O_4@SiO_2 was cooled to room temperature; the product was collected with a magnet and washed with toluene, ethanol–water (1:1, v/v) mixture, and deionized water successively and finally with methanol. The prepared material was dried under vacuum at 60 ºC for 8 h prior to the reaction with N-methylimidazole.[40] The amount of 0.25 g dry Fe_3O_4@SiO_2@CP was placed in a reaction flask containing anhydrous toluene (150 mL) and 5 mL N-methylimidazole (5 mL). The mixture was refluxed with stirring for 48 h. After reflux, the reaction was stopped and the prepared CILMS was cooled to room temperature, and washed with

methanol (2×250 mL) and double distilled water (2×150 mL). The CILMS was dried under vacuum at 50º C for 8 h prior to the characterization or separation.[41]

2.5 Optimization of the parameters that affect the efficiency CILMS separation

2.5.1 The optimization of the nanoparticle concentration

It is required to optimize the nanomaterial concentration in order to achieve high separation performance/capability for CILMS and minimize the cost of the approach. Different volume, (2, 5, 10, 15, 20, 25 μL) of CILMS stock solution (2 mg/mL) were added to the bacteria suspensions. All suspensions were vortexed for 10 min at room temperature. After that the magnetic nanoparticles were separated by an external magnet. CILMS enriched bacteria were washed twice with sterilized and double distilled water in order to remove non-specific interactions. After the removal of liquid portion from the Eppendorf tubes, the nanomaterial was mixed with sinapinic acid matrix (50 mM) before MALDI MS analysis. In order to have a clear justification of the nanoparticle concentration, the control spectra of the pathogenic bacteria were also investigated.

2.5.2 The optimization of incubation time

The incubation period of CILMS with bacteria was examined for 2, 5, 10, 15 and 20 min. The bacterial colonies were suspended in deionized water (DI) after sterilized (1 mL) and the suspension was shaking properly to suspend bacteria uniformly. 10 μL of the well-dispersed stock bacterial suspension was pipetted into five Eppendorf tubes individually. 10 μL of magnetic nanoparticle was added in each Eppendorf tube and replenished the volume up to 1000 μL with the DI water. The Eppendorf tube was maintained for vortex mixing and was taken out individually at the time of 2, 5, 10, 15, and 20 min. An external magnet was applied for the separation of nanoparticles. The materials were washed for two times with DI water thoroughly after collection. Washing is very important to remove the non-specific bounded or free bacteria lysates in the surface of the nanoparticles. After the removal of liquid portion from the Eppendorf tubes, the nanomaterial was

mixed with sinapinic acid (SA) matrix and then spotted onto the MALDI standard plates. The spots were leaved for air-dry before MALDI MS analysis.

2.6 Detection of bacteria in mouse blood

After the bacteria were cultured on the Nutrient Agar plates overnight, a loopful of bacteria was dispersed in an Eppendorf tube with 1 mL phosphate buffer saline (PBS) and labeled as the stock suspension of bacteria. Different volumes (0.5, 1.0, 3.0, 10, 20, 30 μL) of bacterial stock solution were suspended in six different Eppendorf tubes of mice blood solution (1 mL of blood sample (150 μL was diluted to 25 mL)) Then CILMS (10 μL, 2 mg/mL) was added in each Eppendorf tube for bacteria enrichment by applying the nanomaterial. All suspension were vortexed for 5 min, separated by external magnets and then were washed with DI water. The separated particles were mixed with the matrix and spot it in standard plate, dried then were analysis using MALDI-MS.

2.7 The measurement of detection limits

The stock suspension of each bacterium of *E. coli*, *P. aeruginosa* and *S. aureus* was prepared individually. Each strain of bacteria was cultured on the Nutrient Agar plates and used freshly for experiments. Different suspensions (1 mL) of each bacterium with different cells number were prepared. CILMS (10 μL) was added in each Eppendorf tube carefully and vortex for 5 min. After the incubation, the cells were separated using external magnets then were washed with double distilled and sterilized water. The separated CILMS was mixed with SA matrix and spotted on MALDI plate for further analysis.

2.8 The evaluation of bacterial selectivity of CILMS

All three strains of bacteria were cultured on the Nutrient Agar plates separately then were dispersed in deionized and sterilized water. Equal volumes (total volume is 1 mL of different cell

numbers) of the bacterium suspension were mixed in the same Eppendorf tube. CILMS (10 μL, 2 mg/mL) was added and were vortexed for 5 min. After the incubation, an external magnet was applied for separation and washed thoroughly. The three sample mixtures were collected finally from three strains of bacteria. Bacteria mixture was mixed with SA matrix and spotted on the MALDI plate and further MALDI-MS analysis was then performed.

2.9 CILMS assisted MALDI-MS analysis of bacteria in sheep blood

125 μL of sheep blood was diluted with 25 mL double distilled and sterilized water and used as the stock solution for further analysis. Different cell number of three different bacteria suspensions were prepared in sheep blood colloids. CILMS (10 μL, 2 mg/mL) was added to the previous suspension then incubated for 5 mins before separated with external magnets, washed and then mixed with the matrix before MALDI analysis as describe above.

2.10 Transmission electron microscopy (TEM)

To evaluate the affinities of CILMS toward the tested bacteria, TEM analysis was investigated. In a typical procedure, the bacteria cells (1 mL, 10^4–10^5 cfu mL^{-1}) treated with CILMS and were suspended for 30 mins, then were fixed with 2.5% glutaraldehyde for 30 mins. The cells were washed with deionized water, then post-fixed with 1% aqueous OsO_4 (Fluka) for 30 mins and then washed again twice with water. About 10 μL of the mixture was placed on the copper grids and then dried for the TEM measurements.

3. Results and Discussion

3.1 Preparation and characterization of CILMS

The procedure for the synthesis of cationic ionic liquid-modified magnetic nanoparticles (CILMS) and the separation protocol of pathogenic bacteria was illustrated in Scheme 1. Initially, the magnetic nanoparticles (MNPs) were synthesized by the co-precipitation approach. TEM image of the MNPs

reveals that the size is about 20 nm, as shown in Figure 1A. The prepared MNPs were coated by silica layer via the sol-gel method using TEOS as silica source (Scheme 1). The Fe_3O_4@SiO_2 was modified by chloropropyl via reflux using trimethylamine as a catalyst. Immobilized ionic liquid on silica layer was synthesized by treating with 3-chloropropyltrimethoxysilane and followed by reacting with N-methylimidazole. The positive charges on the imidazole rings provide robust electrostatic interaction with negative sites on the surface of pathogens.[42] Due to the paramagnetic Fe_3O_4, the ionic liquid-modified Fe_3O_4@SiO_2 nanoparticles exhibit high reactivity/affinity toward the applied external magnet and can be easily separated from the reaction medium. TEM image (Fig.1B) of Fe_3O_4@SiO_2 shows that the magnetic nanoparticles (Fe_3O_4) are embedded inside the pores of SiO_2. SEM (Fig.1C) and energy dispersive analysis (EDX, Fig.1D) confirms the composition of Fe_3O_4@SiO_2. The FTIR of the prepared materials are shown in Fig. 1E for (a) Fe_3O_4, (b) Fe_3O_4@SiO_2 and (c) CILMS. The peaks at 1090 and 795 cm^{-1} were originated from the Si–O–Si vibrations (spectrum b and c). The band at 2950 cm^{-1} was attributed to the C-H stretch (spectrum c); while the peak at 1660 cm^{-1} refers to -C=N- of imidazole moiety that indicate the ionic portion has been successfully modified onto the Fe_3O_4@SiO_2.

The microbial contamination is a major security issue due to the increasing risk of bioterrorism attacks.[1-26] Recently, MNPs were investigated intensively[7-26] in order to separate and identify the pathogens using many analytical techniques such as UV-Vis absorption, FTIR, fluorescence microscopy, fluorescence spectroscopy, plate counting and MALDI-MS.[7-26] These technologies are simple, easy, inexpensive, and fast. However, they are time consuming, laborious, low sensitivity, require sample pre-treatment and inaccurate. Thus, new approaches are highly required. Beside the facile separation of MNPs using external magnets, they are also easy for surface modification such as ionic liquid (IL). IL may add new functions for MNPs. It could increase the binding forces among the nanoparticles and cells membranes via electrostatic forces that facilitate the

separation and increase the bacteria biomarker during MALDI MS analysis.[23,43] In general, there are two different methods to characterize microorganisms: (1) mass spectra comparison with fingerprints database and (2) matching of biomarker masses to a proteome database. However, the identification faced misidentified mainly due to an incomplete database reference library, database discordances, limit of MALDI-MS resolution, errors in the reference spectra, different aging time, presence of similar spectra in the database, lack of insufficient reference spectra, insufficient protein signals, difficult to lyse cell wall structures, ion suppression due to presence of salts, or other species that has high ionization, and presence of small amount of material samples. In order to reach high separation sensitivity, the influential parameters such as nanoparticle concentration and incubation time were investigated.

3.2 Effect of CILMS concentration on the separation efficiency

The optimization of nanoparticles concentration was investigated using MALDI-MS and the results are shown in Figures 2A, 2B, and S1, for *E.coli*, *P.aeruginosa*, and *S.aureus*, respectively. The results indicated that a minimum of 5 μL CILMS (10 ng mL^{-1}) is required to obtain significant signals for the identification of the bacteria by matching with the control one in (a) of Figures 2A, 2B, S1. In Figure 2A, the main characteristic peaks for *E. coli* (a) such as *m*/*z* 6918, 7401, 8942, 9324, and 9640 Da were found consistently in all samples and were even distinguishable in very low amount of of CILMS (2 μL). In the case of *P. aeruginosa*, as shown in Figure 2B (a), particularly significant peaks such as *m*/*z* 6400.2, 7208.2, 7653.1, 10383.1, and 11890.8 Da can be consistently observed from (b) until (f). In Figure S1 (a), it demonstrates the specific mass peaks such as *m*/*z* 5071, 5569.7, 6677.2, 7169.8, and 8242.9 Da for surface peptide peaks of *S. aureus* can be observed with all quantity of CILMS. Even with 5.0 μL of CILMS is sufficient to get these particular signals. Therefore, 10 μL of CILMS is presumed to be the optimized minimum volume for all the bacteria detection.

3.3 The evaluation of incubation time

The results of variant incubation time (2-20 min) are shown in Figures 3A, 3B, and S2 for *E. coli* (8.1×10^{10} cfu mL^{-1}), *P. aeruginosa* (1.7×10^{10} cfu mL^{-1}) and *S. aureus* (2.9×10^{11} cfu mL^{-1}), respectively. In Figure 3A, it is noteworthy to observe the maximum peaks even with 2 mins of incubation time for *E. coli*. In the case of *P. aeruginosa*, as shown in Figure 3B; most of the peaks from *m*/*z* 2000-14000 can be observed in the period of 2-20 mins. However, the mass signals are prominently observed with 5 mins and longer incubation for *S. aureus* (Figure S2). According to the observations, most of the characteristic peaks were observed even with only 2 mins of incubation and an increasing number of protein peaks were significant with increased incubation time 5 mins and more. Therefore, 5 min of incubation time is sufficient for effective bacteria capture.

3.4 MALDI-MS analysis of bacteria in real samples from mice blood

Analysis of pathogenic bacteria in real samples such as blood is a great challenge due to the intensive interferences of blood such as cells, metals, proteins and extremely low number of pathogenic bacteria.[17, 22, 44, 45] Therefore, pre-concentration and sample pretreatment are necessary. Bacteria are difficult to be detected in blood by MALDI-MS and require enrichment, and sample pretreatment prior to analysis. Nanoparticles typically can improve the bacteria detection due to their large surface area and small volume ratios. MALDI-MS spectra of *E. coli* (4.8×10^{10} cfu mL^{-1}), *P. aeruginosa* (9.87×10^{10} cfu mL^{-1}) and *S. aureus* (7.89×10^{13} cfu mL^{-1}) in mice blood samples are shown in Figures 4A, 4B and supporting Figure S4, respectively. The marked asterisks represent peaks originated from mice blood, and (a), (b) in each figure is for blood and bacterial control, respectively. The characteristic protein peaks from mice blood are labelled by asterisks (*). MALDI-MS spectra show clearly the characteristic peaks of each bacterium. The direct observation of the bacterium indicates the superior of the proposed assay over than the other analytical techniques that give indirect

assessment. According to these observations, it reveals that even in complex matrix like blood samples, CILMS are capable to detect the mass signals of bacteria and further enrich the mass signals effectively.

After the optimization of CILMS volume, incubation time, the lowest detectable bacterial colony by the application of the nanomaterial was investigated. The LOD investigation for *E. coli*, *P. aeruginosa* and *S. aureus* are shown in Fig. 5A, 5B, and S5 respectively. For *E. coli*, the concentrations were prepared as (a) 2.7×10^2, (b) 3.4×10^3, (c) 4.2×10^3, (d) 6.5×10^5, (e) 7.1×10^6, (f) 8.4×10^7, and (g) 9.1×10^8 cfu mL^{-1} in Figure 5A. The lowest colony detected is 3.4×10^3 cfu mL^{-1} in Fig. 5A (b) since the characteristic peaks. Moreover, the peaks were even as significant as high count of bacteria. In the case of *P. aeruginosa*, the concentrations were prepared as (a) 2.5×10^2, (b) 3.2×10^3, (c) 5.2×10^5, (d) 6.9×10^6, (e) 7.5×10^7, (f) 8.2×10^8, and (g) 9.6×10^9 cfu mL^{-1} in Fig. 5B. The lowest colony count detected is 3.2×10^3 cfu mL^{-1} as the bacterial peaks exhibited sharply in high intensity, as shown in Fig. 5B(b). However, significant signals are hardly observed for the counts lower than 10^2 cfu mL^{-1}. As for *S. aureus*, the lowest colony detected is 4.2×10^3 cfu mL^{-1} and the signals of *S. aureus* are prominent as shown in Figure S5(b). Thus, this count can be perceived as the limit of detection of *S. aureus*. The low concentration is due to the large surface area/volume ratios of CILMS which can effectively enhance the bacteria detection. This type of approach in reality/nature belongs to the surface assisted laser desorption/ionization mass spectrometry (SALDI-MS).

3.5 The evaluation of bacterial selectivity of CILMS

Selective analysis of pathogenic bacteria is far more difficult in MALDI-MS, because the system is complicated and they contain various types of biomolecules. However, the selectivity of CILMS toward particular bacterium among these three species was conducted, which is shown in Fig. S3. The control concentrations of the bacteria were (a) *S. aureus* (1.7×10^{13} cfu mL^{-1}), (b) *P. aeruginosa* (3.6×10^{13} cfu mL^{-1}) and (c) *E. coli* (4.1×10^{13} cfu mL^{-1}) in Figure S3. MALDI-MS spectra of the

bacterial mixtures for (*P. aeruginosa* & *S. aureus*), (*E. coli* & *S. aureus*, and (*E. coli* & *P. aeruginosa*) are shown in Fig. S3 (d), (e), and (f), respectively. Among these bacteria, a substantial number of signals were observed in (d) and (f) for *P. aeruginosa*. Compared with *P. aeruginosa*, fewer number of signals were observed in (d), (e) for *S. aureus* and (e), (f) for *E. coli*. From all the spectra observed, it can be concluded that the enrichment capacity of CILMS toward these bacteria is in the order of *P. aeruginosa* > *S. aureus* > *E. coli*. It is important to note that ion suppression play as significant role to govern the selectivity of the detection. It is also function on the ionizability that varies between the different analytes. Thus, direct comparisons between the different analytes are taught.

3.6 MALDI-MS analysis of bacteria in real samples from sheep blood

The application of CILMS toward bacteria was further applied for another real sample: the sheep blood for *E. coli* (8.5×10^{12} cfu mL^{-1}), *P. aeruginosa* (1.7×10^{13} cfu mL^{-1}) and *S. aureus* (7.5×10^{13} cfu mL^{-1}), as shown in Figure S6(A), (B), (C) respectively. The asterisks in spectra indicate the signals were originated from blood. The number and intensity of peaks increased without considerable interferences in the bacterial analysis from the sheep blood samples, which is in accordance with the increasing concentrations of bacteria.

3.7 Mechanistic study of the bacteria separation of CILMS using TEM analysis

As alluded above, the bacterial capture is influenced by the charges of bacteria surface and surface of CILMS. CILMS captures the bacteria cells mainly by the attractive electrostatic interaction among the negatively charged bacteria and the positively charged of CILMS surface. Bacterial cell surfaces possess net negative electrostatic charges due to ionized phosphoryl and carboxylate substituent on outer cell envelope macromolecules or due to techoic acid of Gram positive and lipopolysaccharide in Gram negative.[12] The predominantly negative surface charges of the bacterial cellular membranes provides a clear target for separation via electrostatic interactions with CILMS.[46] However, the pendant propyl moiety offers also hydrophobic interaction toward the pathogenic bacteria. The

hydrophobic interactions play a supplementary role in the separation process. In order to investigate these affinities, TEM analysis (Figure 6) of the bacteria cells (A) *P. aeruginosa*, (B) *S. aureus* and (C) *E. coli* before (a) and after (b) interaction with CILMS was reported. TEM images show the high affinity of the different bacteria to CILMS that immobilized on the cell membrane thus facilitates the separation (Fig.1A).

A comparison of the present method with other methods for capturing bacteria by the functional magnetic nanoparticles is tabulated in Table 1. It reveals that the present method offer a lot of merits such as simple surface modification, fast, and high capture efficiency. The detection method such as plate counting, microscopy requires long time for incubation or observation (Table 1). In contrast, MALDI MS is a fast technique as analysis of separated bacteria cells required only few micro liters. The sample analysis of bacteria sample in the clinical field by MALDI MS is approximately 10 – 20 times cheaper than the analysis by conventional methods. [47] It also can identify the bacteria cells based on their biomarker peaks or protein profiles.[47, 48] MALDI MS can provide three types of characterization at the strain level: (1) strain categorization, (2) strain differentiation, and (3) strain identification.[47, 48] The biomolecules of the intact cells are lysed physically (e.g., sonication,[44] vortexed, or other physical methods) or chemically (e.g., via exposure to organic matrices, or TFA or formic acid/organic solvents that were used during the matrix preparation). These process release the contents of the cells into the supernatant, thus it can be detected during MALDI MS analysis. The large surface area/volume ratios of magnetic nanoparticle encourage these process, thus it improve the detection. Comparing with other extraction methods such as liquid- liquid microextraction, CILMS provide a simple, effective, selective, sensitive and environmental friendly (Table 2). As no toxic solvent are used and no further equipment are required. Although fluorescence measurements are very sensitive, they are not convenient for real-time on-site applications due to the requirement for bulky instrumentation and labelling with suitable fluorophore. The latter requirement is also

important for UV-Vis absorption spectrometer that requires a chromophore such as gold nanoparticles or TiO_2 nanocrystals[49]. Due to this requirement, UV detection is expensive and lack of sensitivity and selectivity. Recently, Lee reported magnetic nanoparticles (MNPs) modified with a synthetic ligand, zinc-coordinated bis(dipicolylamine) (bis-Zn-DPA), that can be utilized for highly selective and rapid separation of bacteria and potentially their endotoxins from whole blood using a magnetic microfluidic device[50]. The magnetic nanoparticles (MNPs) were also applied to adsorb genome DNA after the bacteria were lysed. Then the DNA@MNPs was directly subjected to polymerase chain reaction (PCR) to amplify gyrB specific sequence of *P. aeruginosa*. However, it is highly selective, but the signal must amplify because the weak signal of DNA[5].

4. Conclusions

A simple, rapid, direct and cost-effective assay was developed by combining ionic liquid magnetic nanoparticles and MALDI mass spectrometry for the detection of pathogens in blood samples. The functional magnetic nanoparticles were synthesized from co-precipitation of ferrous and ferric salts, the core-shell Fe_3O_4@SiO_2 nanoparticles were prepared by the sol-gel process and followed by the grafting of 3-chloropropyltrimethoxysilane on the nanoparticles and reacted further with N-methylimidazole. Our detection method possesses many advantages over those conventional methods; the measurement is rapid because it does not require cell culturing; cheap as expensive nanoparticles are avoided; highly sensitive (3.4×10^3, 3.2×10^3, and 4.2×10^3 cfu mL^{-1} for *E. coli*, *P. aeruginosa*, and *S. aureus*, respectively); and direct as the proteomic analysis were investigated using MALDI-MS that give a fingerprint of each strain. The present assay can be applied effectively for blood sample which contain intensive interferences such as blood cells (RBC), salts and proteins.

Acknowledgements

The authors are particularly grateful to the Ministry of Science and Technology of Taiwan for financial support.

References

1. H. Gu, P.-L. Ho, K. W. T. Tsang, L. Wang and B. Xu, J Am Chem Soc, 2003, **125**, 15702-15703.
2. K. C. Ho, P. J. Tsai, Y. S. Lin and Y. C. Chen, Anal. Chem, 2004, **76**, 7162-7168.
3. Y.-S. Lin, P.-J. Tsai, M.-F. Weng and Y.-C. Chen, Anal. Chem, 2005, **77**, 1753-1760.
4. J. C. Liu, W. J. Chen, C. W. Li, K. K. Mong, P. J. Tsai, T. L. Tsai, Y. C. Lee and Y. C. Chen, The Analyst, 2009, **134**, 2087-2094.
5. Y. Tang, J. Zou, C. Ma, Z. Ali, Z. Li, X. Li, N. Ma, X. Mou, Y. Deng, L. Zhang, K. Li, G. Lu, H. Yang and N. He, *Theranostics*, 2013, **3**, 85-92.
6. X. Zhang, X. He, L. Chen, Y. Zhang, J. Mater. Chem. B, 2014 DOI: 10.1039/c4tb00379a
7. H. Honda, A. Kawabe, M. Shinkai and T. Kobayashi, J. fermen. bioengineering, 1998, **86**, 191-196.
8. C.-C. Lin, Y.-C. Yeh, C.-Y. Yang, C.-L. Chen, G.-F. Chen, C.-C. Chen and Y.-C. Wu, J. Amer. Chem. Soc, 2002, **124**, 3508-3509.
9. K. Tsang, Chem. Comm, 2003, 1966-1967.
10. X. Zhao, L. R. Hilliard, S. J. Mechery, Y. Wang, R. P. Bagwe, 1 S. Jin and W. Tan, Proc. Natl. Acad. Sci. U.S.A. 2004, **101**, 15027-15032.
11. S. Yitzhaki, E. Zahavy, C. Oron, M. Fisher and A. Keysary, Anal. Chem, 2006, **78**, 6670-6673.
12. K. El-Boubbou, C. Gruden and X. Huang, J. Am. Chem. Soc, 2007, **129**, 13392-13393.
13. M. Varshney and Y. Li, Biosens. Bioelectron, 2007, **22**, 2408-2414.
14. W.-J. Chen, P.-J. Tsai and Y.-C. Chen, Anal. Chem, 2008, **80**, 9612-9621.
15. A. J. Kell, K. Somaskandan, G. Stewart, M. G. Bergeron and B. Simard, Langmuir, 2008, **24**, 3493-3502.

16. A. J. Kell, G. Stewart, S. Ryan, R. Peytavi, M. Boissinot, A. Huletsky, M. G. Bergeron and B. Simard, *ACS Nano*, 2008, **2**, 1777-1788.
17. J.-C. Liu, P.-J. Tsai, Y. C. Lee and Y.-C. Chen, Anal. Chem, 2008, **80**, 5425-5432.
18. L. Bromberg, S. Raduyk and T. A. Hatton, Anal. Chemistry, 2009, **81**, 5637-5645.
19. J. Gao, H. Gu and B. Xu, *Acc. Chem. Res*, 2009, **42**, 1097-1107.
20. L.-H. Liu, H. Dietsch, P. Schurtenberger and M. Yan, *Bioconjugate Chem*, 2009, **20**, 1349-1355.
21. S. Ryan, A. J. Kell, H. van Faassen, L.-L. Tay, B. Simard, R. MacKenzie, M. Gilbert and J. Tanha, *Bioconjugate Chem*, 2009, **20**, 1966-1974.
22. X. Pei, Y. H. Yan, L. Yan, P. Yang, J. Wang, R. Xu and M. B. Chan-Park, Carbon, 2010, **48**, 2501-2505.
23. Z. Shan, Q. Wu, X. Wang, Z. Zhou, K. D. Oakes, X. Zhang, Q. Huang and W. Yang, Anal. Biochem, 2010, 398, 120-122.
24. H. N. Abdelhamid and H.-F. Wu, J. Mater. Chem. B, 2013, **1**, 3950-3961.
25. H. J. Chung, C. M. Castro, H. Im, H. Lee and R. Weissleder, Nat Nano, 2013, **8**, 369-375.
26. Y. Zhang and C. Xia, Applied Catalysis A: General, 2009**, 1**, 366, 141-147.
27. J. Safari and Z. Zarnegar, Comptes Rendus Chimie, 2013, **16**, 821-828.
28. R. Linhardt, Q. M. Kainz, R. N. Grass, W. J. Stark, O. Reiser, RSC Adv., 2014, **4**, 8541
29. S. Sobhani and M. Honarmand, Applied Catalysis A: General, 2013, **467**, 456-462.
30. G. Absalan, M. Asadi, S. Kamran, L. Sheikhian and D. M. Goltz, Journal of hazardous materials, 2011, **192**, 476-484.
31. H. Bagheri, R. Daliri and A. Roostaie, Anal, chim. Acta, 2013, **794**, 38-46.
32. C. Barrera, A. Herrera, Y. Zayas and C. Rinaldi, J. Magn. and Magn. Mater, 2009, **321**, 1397-1399.

33. W. Sun, Z. Sun, L. Zhang, X. Qi, G. Li, J. Wu and M. Wang, Colloids and Surfaces B: Biointerfaces, 2013, **101**, 177-182.
34. 34. Y. Wei, Y. Li, A. Tian, Y. Fan and X. Wang, J. Mater. Chem. B, 2013, **1**, 2066.
35. H. Gu, K. Xu, C. Xu and B. Xu, Chem.Commun, 2006, 941-949.
36. C.-T. Chen and Y.-C. Chen, J. Mass Spectrom, 2008, 43, 538-541.
37. S. P. Ravindranath, L. J. Mauer, C. Deb-Roy and J. Irudayaraj, Anal. Chem, 2009, **81**, 2840-2846.
38. J. Gopal, H. N. Abdelhamid, P.-Y. Hua and H.-F. Wu, J. Mater. Chem. B, 2013, 1, 2463-2475.
39. G. Gnanaprakash, S. Ayyappan, T. Jayakumar, J. Philip and B. Raj, Nanotechnology, 2006, **17**, 5851-5857.
40. L. M. L. A. Auler, C. R. Silva, K. E. Collins and C. H. Collins, J. Chromatog. A, 2005, 1073, 147-153.
41. H. Qiu, S. Jiang and X. Liu, J. Chromatogr. A, 2006, 1103, 265-270.
42. Y.-F. Huang, Y.-F. Wang and X.-P. Yan, Environ. Sci.Techn, 1 2010, 44, 7908-7913.
43. (a) H. N. Abdelhamid, J. Gopal and H.-F. Wu, Anal. Chim. Acta, 2013, **767**, 104-111; (b) H. N. Abdelhamid, M. S. Khan, H.F. Wu, Analytica Chimica Acta, 2014, **823**, 51–60
44. H. N. Abdelhamid, M. L. Bhaisare and H.-F. Wu, Talanta, 2014, **120**, 208-217.
45. H. N. Abdelhamid and H.-F. Wu, Colloids and Surfaces B: Biointerfaces, 2014, **115**, 51-60.
46. W. W. Wilson, M. M. Wade, S. C. Holman and F. R. Champlin, Jo.Microbiolog. Methods, 2001, **43**, 153-164.
47. (a) A. Cherkaoui, J. Hibbs, S. Emonet, M. Tangomo, M. Girard, P. Francois, J. Schrenzel, J. Clin. Microb.2010, **48,** 1169–1175. (b) M. Welker, *Proteomics*, 2011, **11**, 3143-3153.

48. (a) T. R. Sandrin, J. E. Goldstein and S. Schumaker, Mass Spectrometry Reviews, 2013, 32, 188-217. (b) L. Krasny, R. Hynek, I. Hochel, Inter. J. Mass Spectrom.2013, **353**, 67 – 79

49. (a) J. Joo, C. Yim, D. Kwon, J. Lee, H. H. Shin, H.J. Cha, S. Jeon, Analyst, 137 (2012) 3609–3612, ((b) Y. J.Sung , H. J.Suk , H.Y. Sung , T. Li , H. Poo , M.G. Kim, *Biosen.Bioelectron.*43 (2013) 432–439

50. J.J. Lee, K. J. Jeong, M.Hashimoto, A.H. Kwon, A. Rwei, S. A. Shankarappa, J. H. Tsui, D. S. Kohane, *Nano Lett*. 14 (2014) 15

Figure captions

Scheme 1: Schematic illustrations for the preparation of CILMS and the capture of bacteria by the magnetic nanoparticles. Optical images represent the nanoparticle before (left) and after (right) separation

Fig. 1. Characterization of CILMS using TEM images of (A) Fe_3O_4 and (B) Fe_3O_4@SiO_2; (C) SEM, (D) EDX analysis and (D) FT-IR spectra.

Fig. 2. (A) Volume effects of CILMS on capture of *E. coli* with (a) bacteria control, (b) 2.0, (c) 5.0, (d) 10, (e) 15, (f) 20, and (g) 25 μL CILMS. (B) the same conditions with *P. aeruginosa*.

Fig. 3. (A) Incubation time effect on capture of *E. coli* (8.1×10^{10} cfu mL^{-1}) with 10 μL CILMS (a) bacteria control, after (b) 2, (c) 5, (d) 10, (e) 15, and (f) 20 min incubation. (B) The same conditions with *P. aeruginosa* (1.7×10^{10} cfu mL^{-1}).

Fig. 4. (A) The evaluation of *E. coli* capture in mice blood sample with CILMS and (a) blood control, (b) bacteria control, (c) 0.5, (d) 1.0, (e) 3.0, (f) 10 (g) 20, and (h) 30 μL *E. coli* (4.8×10^{10} cfu mL^{-1}). (B) The same conditions with *P. aeruginosa* (9.8×10^{12} cfu mL^{-1}).

Fig. 5. (A) LOD determination of *E. coli* from (a) 2.7×10^{2}, (b) 3.4×10^{3}, (c) 4.2×10^{3}, (d) 6.5×10^{5}, (e) 7.1×10^{6}, (f) 8.4×10^{7}, and (g) 9.1×10^{8} cfu mL^{-1} *E. coli* with CILMS, and (B) for *P. aeruginosa* from (a) 2.5×10^{2}, (b) 3.2×10^{3}, (c) 5.2×10^{5}, (d) 6.9×10^{6}, (e) 7.5×10^{7}, (f) 8.2×10^{8}, and (g) 9.6×10^{9} cfu mL^{-1} *P. aeruginosa*.

Fig.6. TEM analysis of the bacteria cells (A) *P. aeruginosa*, (B) *S. aureus* and (C) *E. coli* before (a) and after (b) interaction with CILMS.

Table1: Comparison among the different MNPs that were used for pathogenic bacteria detections

No	**MNPs**	**Bacteria**	**Incubation time min**	**Detection Methods**	**LOD (CFU mL^{-1})**	**Ref.**
1	CILMS	*E. coli, S, aureus, P. aeruginosa*	5	MALDI-MS	3.4×10^{3}, 3.2×10^{3}, and 4.2×10^{3} cfu mL^{-1} for *E. coli*, *P. aerugin osa*, and	Here

					S. aureus, respectively	
3	FePt-Vancomycin	*E. Coli*	10	Microscopy	15	35
5	antibody-nanoparticle	*S. aureus*	10	Flow cytometry	ND	21
6	antibody-conjugated magnetic nanoparticles (MNPs) and TiO2 nanocrystals (TNs)	*Salmonella*	20 mins	UV	100 cfu mL^{-1}	49 (a)
7	antibody/gold nanoparticle/ magnetic nanoparticle nanocomposites (anti-body/AuNP/ MNPs)	*S. aureus*	40 min	Colorimetric detection	1.5×10^{3} and 1.5×10^{5} CFU in PBS and the milk sampler espectively	49 (b)
8	Fe_3O_4@SiO_2	*P. aeruginosa*	60 mins	*in situ* PCR	10 $cfu.mL^{-1}$	5

1

1 **Table 2**: Comparison between different techniques that used to extract and identify bacteria

Technique	**Bacteria**	**Materials**	**LOD**	**Ref.**
Affinity probes	*S. marcescens and E. coli*	Immunoglobulin immobilized on platinum nanoparticles	10^5	11
Direct detection	*S. aureus and P. aeruginosa*	Ionic liquid matrices	10^4-10^5	43
UESA-DLLME	*S. aureus and P. aeruginosa*	CeO_2@CTAB	10^4	47
MALDI-MS	*S. aureus, P. aeruginosa and E. coli*	Fe_3O_4@SiO_2	10^3	This work

2 UESA-DLLME: Ultrasonic enhanced surfactant assisted dispersive liquid-liquid microextraction

3

Scheme 1

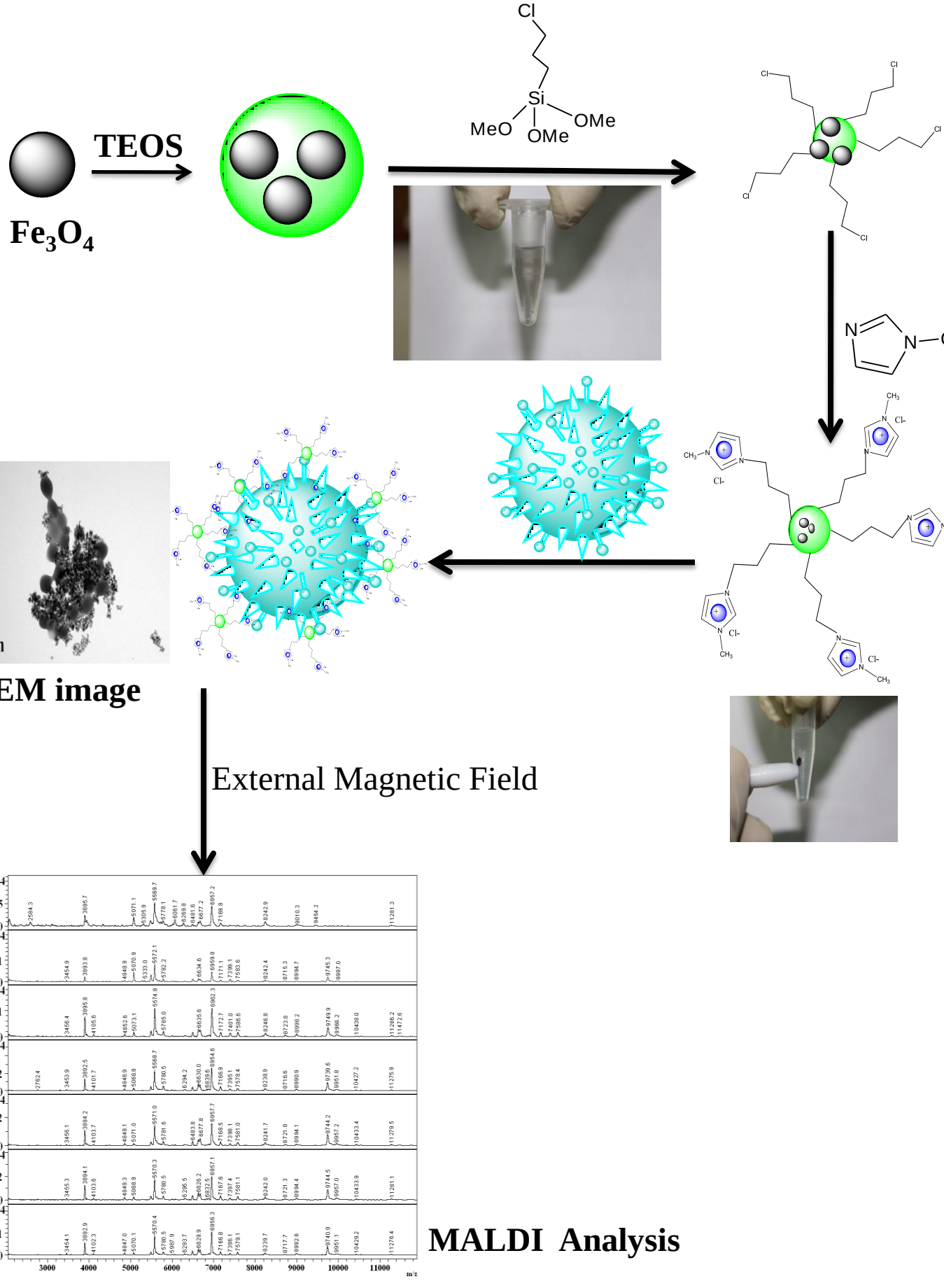
TEOS
Fe_3O_4
Cl
Si
MeO
OMe
OMe
Cl
Cl
Cl
Cl
Cl
N
N
CH_3
Cl-
1 μm
TEM image
External Magnetic Field
MALDI Analysis

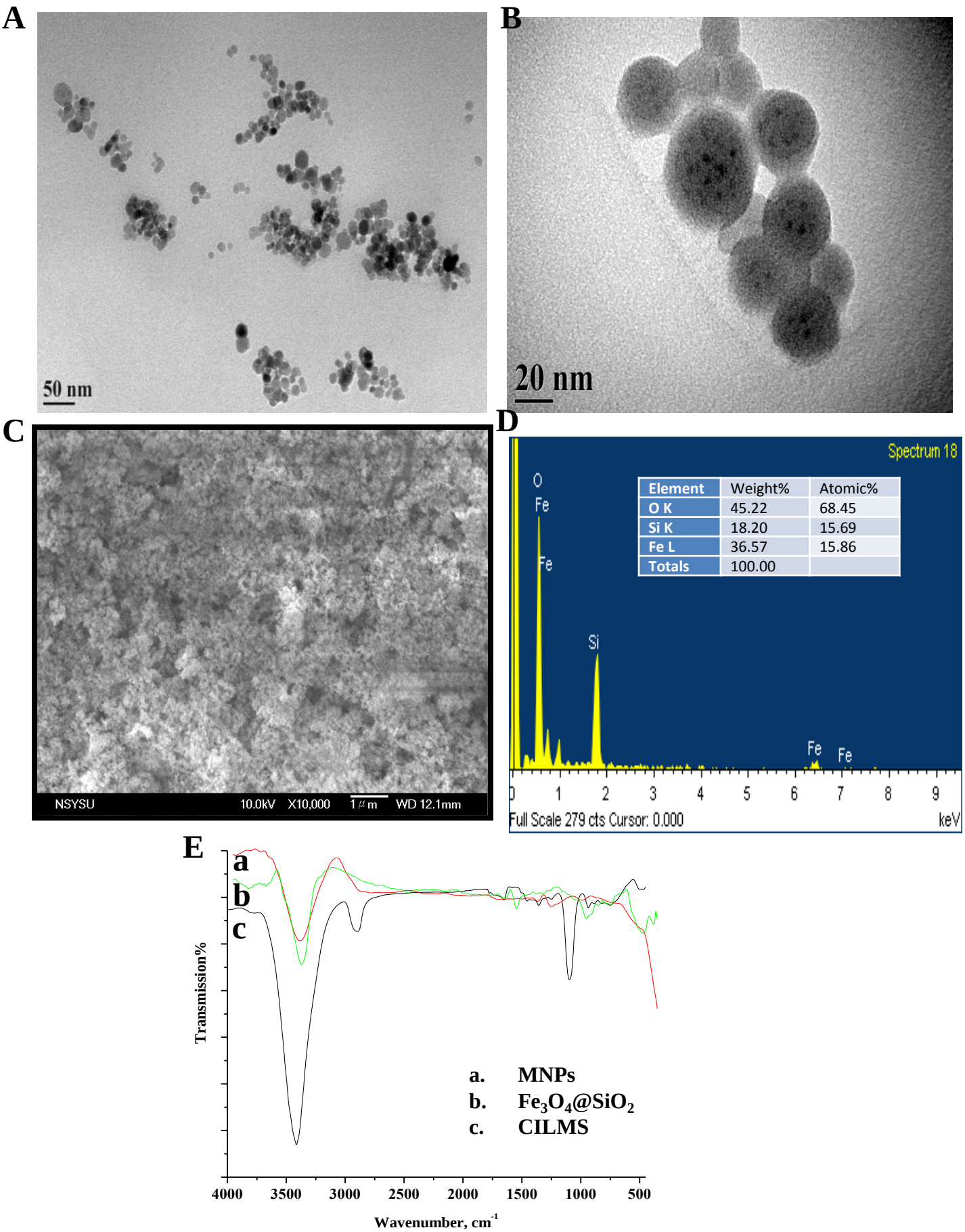
A
50 nm
B
20 nm
C
NSYSU 10.0kV X10,000 1μm WD 12.1mm
D
Spectrum 18
O
Fe
Fe
Si
Fe
Fe
Element | Weight% | Atomic%
O K | 45.22 | 68.45
Si K | 18.20 | 15.69
Fe L | 36.57 | 15.86
Totals | 100.00
0 1 2 3 4 5 6 7 8 9
Full Scale 279 cts Cursor: 0.000
keV
E
a
b
c
Transmission%
a. MNPs
b. Fe3O4@SiO2
c. CILMS
4000 3500 3000 2500 2000 1500 1000 500
Wavenumber, cm-1

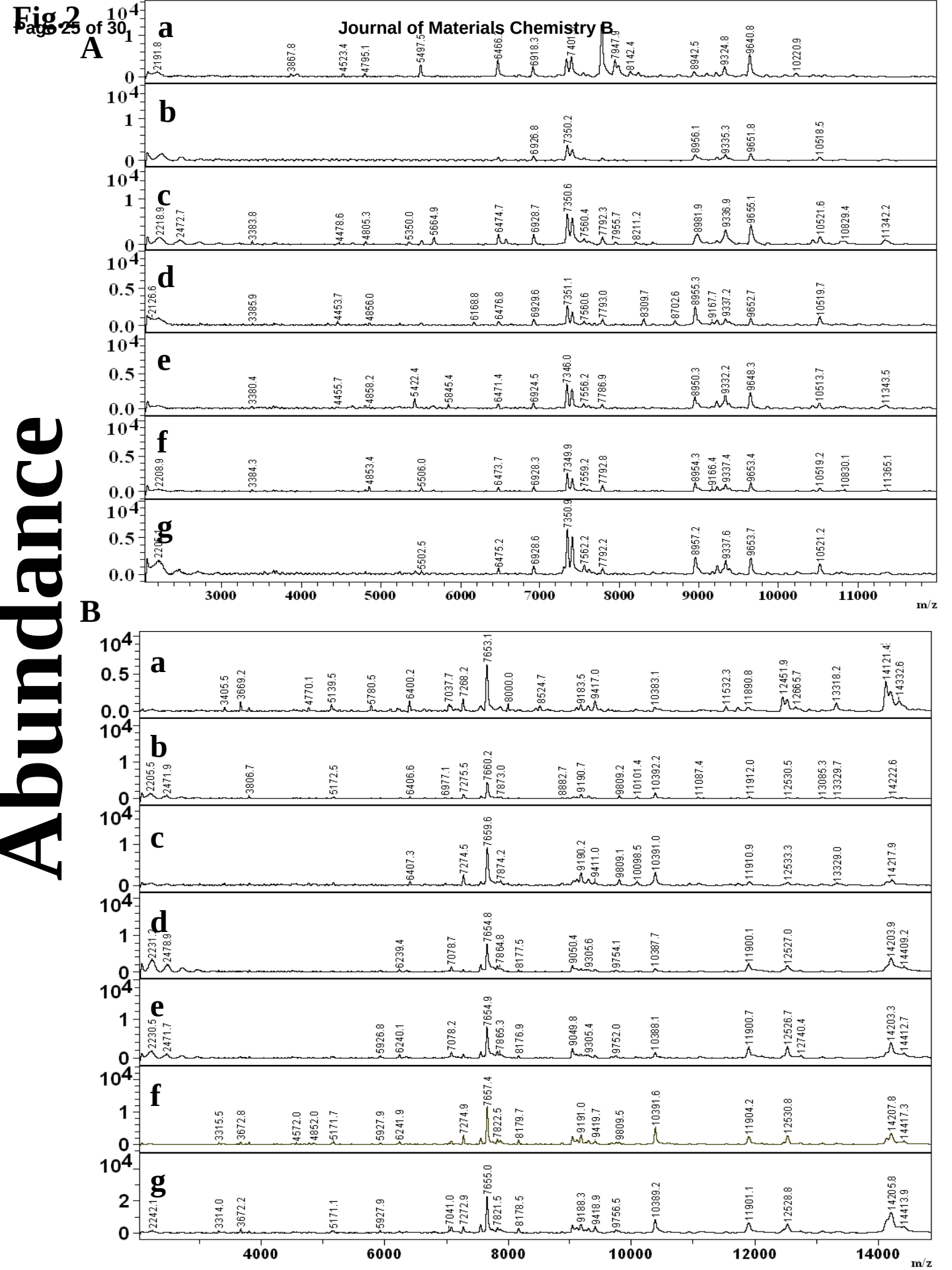
A
B
Abundance
a
b
c
d
e
f
g
m/z
3000
4000
5000
6000
7000
8000
9000
10000
11000
12000
14000

Fig.3

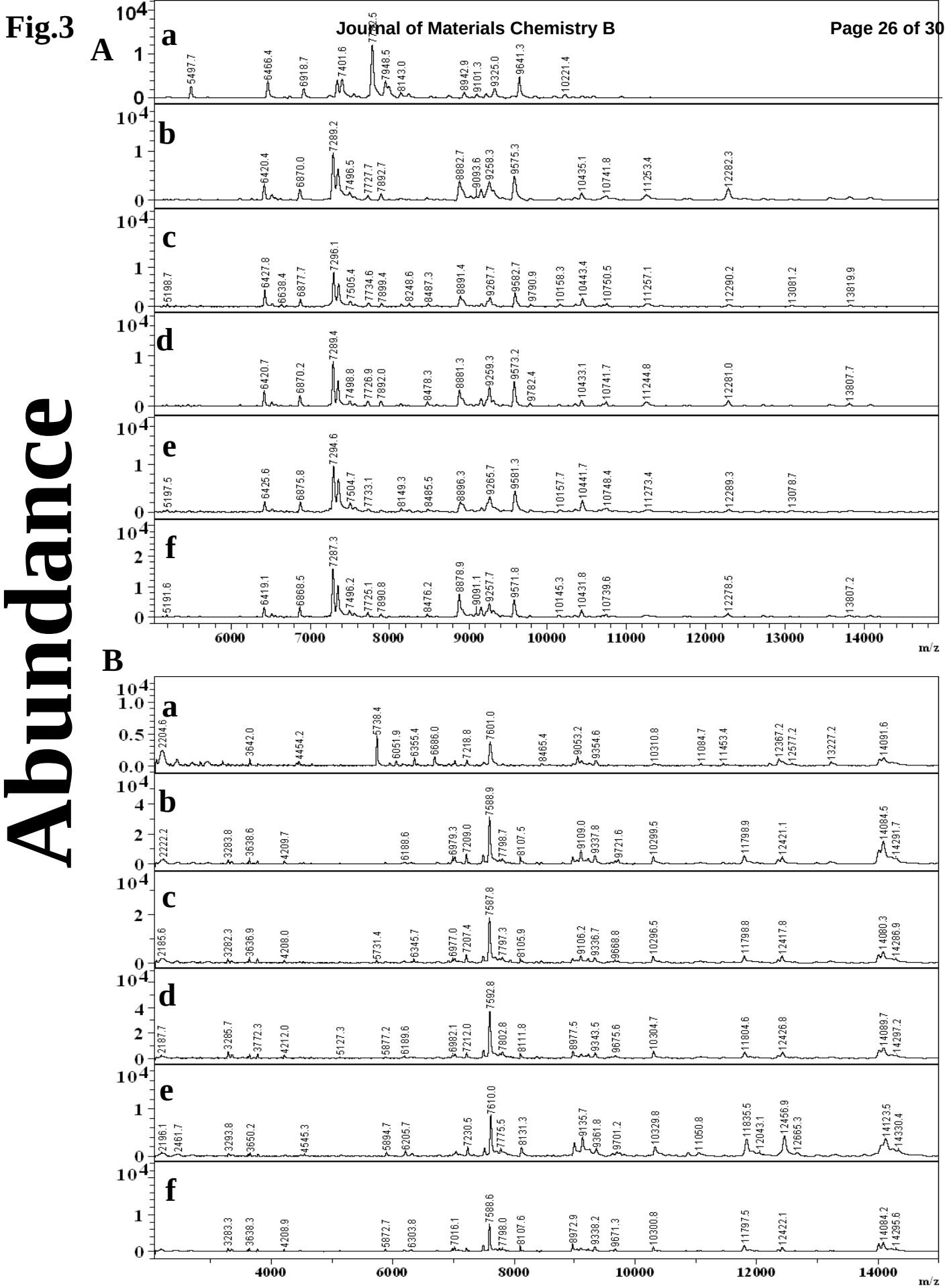
A
B
Abundance
m/z
a
b
c
d
e
f
5497.7
6466.4
6918.7
7401.6
7948.5
8143.0
8942.9
9101.3
9325.0
9641.3
10221.4
6420.4
6870.0
7289.2
7496.5
7727.7
7892.7
8882.7
9093.6
9258.3
9575.3
10435.1
10741.8
11253.4
12282.3
5198.7
6427.8
6638.4
6877.7
7296.1
7505.4
7734.6
7899.4
8248.6
8487.3
8891.4
9267.7
9582.7
9790.9
10158.3
10443.4
10750.5
11257.1
12290.2
13081.2
13819.9
6420.7
6870.2
7289.4
7498.8
7726.9
7892.0
8478.3
8881.3
9259.3
9573.2
9782.4
10433.1
10741.7
11244.8
12281.0
13807.7
5197.5
6425.6
6875.8
7294.6
7504.7
7733.1
8149.3
8485.5
8896.3
9265.7
9581.3
10157.7
10441.7
10748.4
11273.4
12289.3
13078.7
5191.6
6419.1
6868.5
7287.3
7496.2
7725.1
7890.8
8476.2
8878.9
9091.1
9257.7
9571.8
10145.3
10431.8
10739.6
12278.5
13807.2
6000
7000
8000
9000
10000
11000
12000
13000
14000
2204.6
3642.0
4454.2
5738.4
6051.9
6355.4
6686.0
7218.8
7601.0
8465.4
9053.2
9354.6
10310.8
11084.7
11453.4
12367.2
12577.2
13227.2
14081.6
2222.2
3283.8
3638.6
4209.7
6188.6
6979.3
7209.0
7588.9
7798.7
8107.5
9109.0
9337.8
9721.6
10299.5
11798.9
12421.1
14084.5
14291.7
2185.6
3282.3
3636.9
4208.0
5731.4
6345.7
6977.0
7207.4
7587.8
7797.3
8105.9
9106.2
9336.7
9668.8
10296.5
11798.8
12417.8
14080.3
14286.9
2187.7
3285.7
3772.3
4212.0
5127.3
5877.2
6189.6
6982.1
7212.0
7592.8
7802.8
8111.8
8977.5
9343.5
9675.6
10304.7
11804.6
12426.8
14089.7
14297.2
2196.1
2461.7
3293.8
3650.2
4545.3
5894.7
6205.7
7230.5
7610.0
7775.5
8131.3
9135.7
9361.8
9701.2
10329.8
11050.8
11835.5
12043.1
12456.9
12665.3
14123.5
14330.4
3283.3
3638.3
4208.9
5872.7
6303.8
7016.1
7588.6
7798.0
8107.6
8972.9
9338.2
9671.3
10300.8
11797.5
12422.1
14084.2
14295.6
4000
6000
8000
10000
12000
14000

Fig. 4

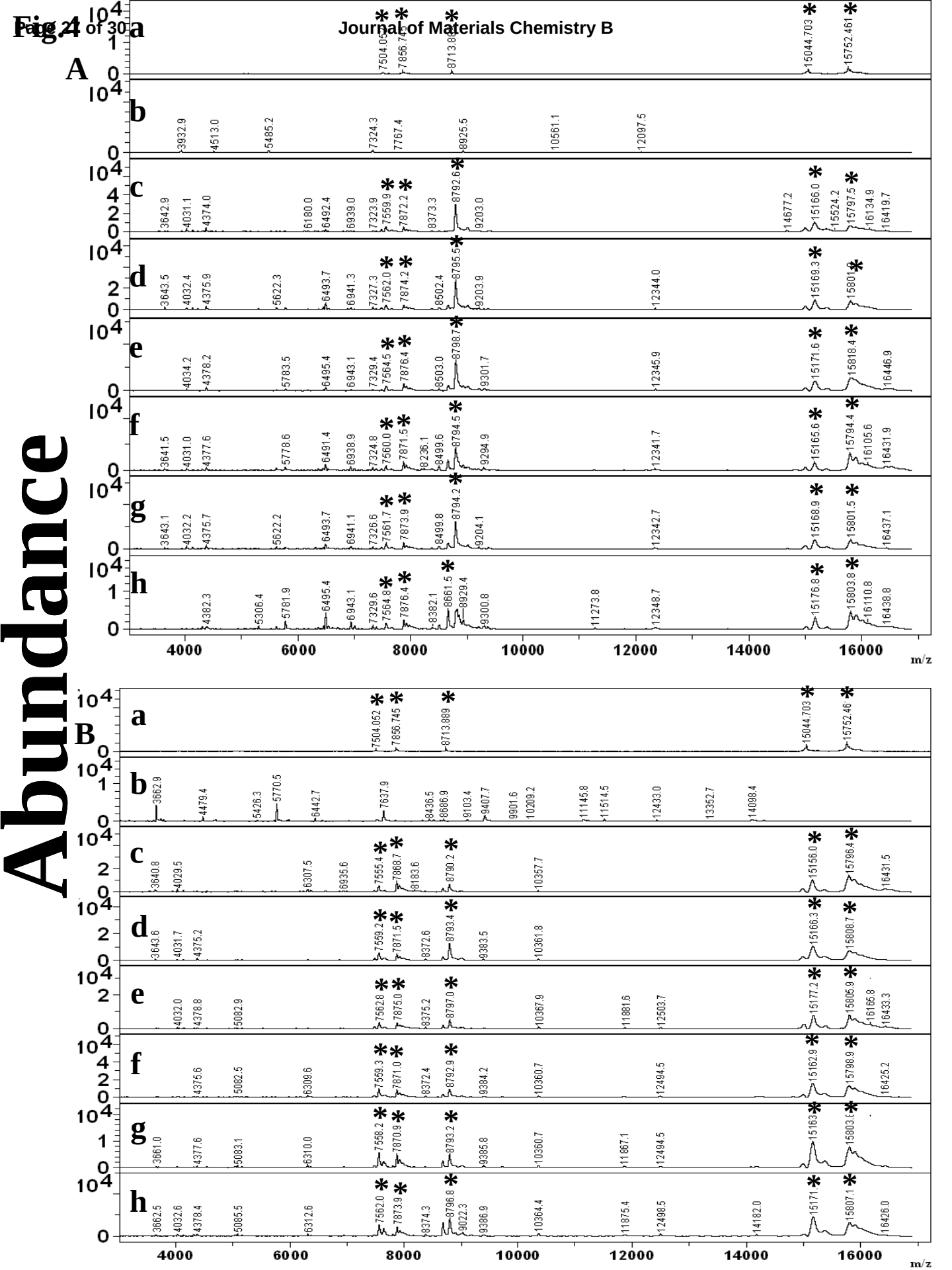

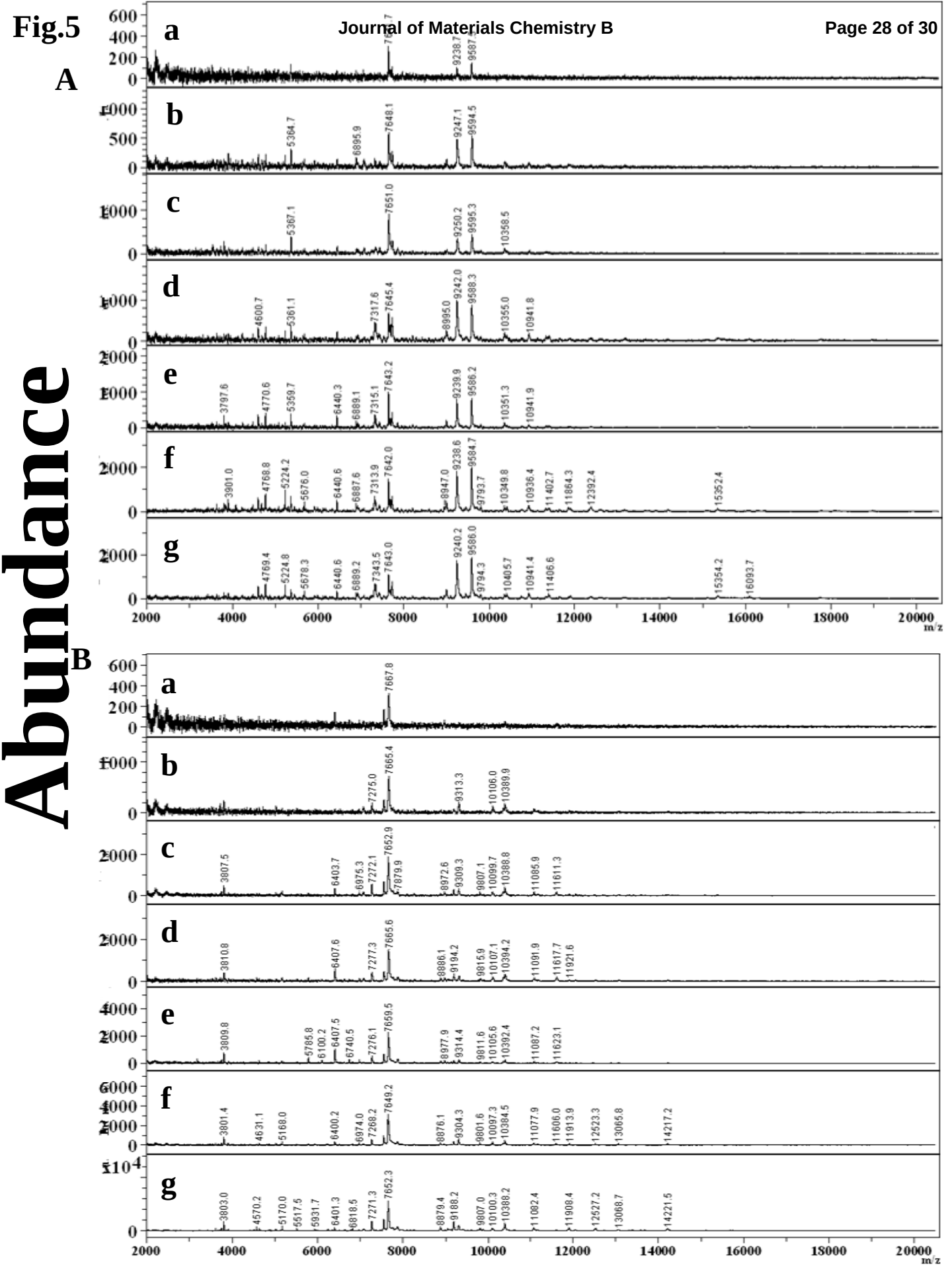
A
B
Abundance
a
b
c
d
e
f
g
m/z
7667.8
7665.4
7275.0
9313.3
10106.0
10389.9
3807.5
6403.7
6975.3
7272.1
7652.9
7879.9
8972.6
9309.3
9807.1
10099.7
10388.8
11085.9
11611.3
3810.8
6407.6
7277.3
7665.6
8886.1
9194.2
9815.9
10107.1
10394.2
11091.9
11617.7
11921.6
3809.8
5785.8
6100.2
6407.5
6740.5
7276.1
7659.5
8977.9
9314.4
9811.6
10105.6
10392.4
11087.2
11623.1
3801.4
4631.1
5168.0
6400.2
6974.0
7268.2
7649.2
8876.1
9304.3
9801.6
10097.3
10384.5
11077.9
11606.0
11913.9
12523.3
13065.8
14217.2
3803.0
4570.2
5170.0
5617.5
5931.7
6401.3
6818.5
7271.3
7652.3
8879.4
9188.2
9807.0
10100.3
10388.2
11082.4
11908.4
12527.2
13068.7
14221.5

Fig.6